Structural Engineering and Mechanics, Vol. 7, No. 2 (1999) 203-216
DOI: http://dx.doi.org/10.12989/sem.1999.7.2.203

A simple method of stiffness matrix formulation based on single element test

S.T. Mau†

Newark College of Engineering, New Jersey Institute of Technology, Newark, NJ 07102, U.S.A.

Abstract. A previously proposed finite element formulation method is refined and modified to generate a new type of elements. The method is based on selecting a set of general solution modes for element formulation. The constant strain modes and higher order modes are selected and the formulation method is designed to ensure that the element will pass the basic single element test, which in turn ensures the passage of the basic patch test. If the element is to pass the higher order patch test also, the element stiffness matrix is in general asymmetric. The element stiffness matrix depends only on a nodal displacement matrix and a nodal force matrix. A symmetric stiffness matrix can be obtained by either modifying the nodal displacement matrix or the nodal force matrix. It is shown that both modifications lead to the same new element, which is demonstrated through numerical examples to be more robust than an assumed stress hybrid element in plane stress application. The method of formulation can also be used to arrive at the conforming displacement and hybrid stress formulations. The convergence of the latter two is explained from the point of view of the proposed method.

Key words: patch test; convergence; element formulation; asymmetric stiffness matrix; higher order performance.

1. Introduction

In the history of finite element development, the invention of the classical patch test by Irons (Bazeley *et al.* 1966, Irons and Razzaque 1972) certainly ranks as one of the most important events. The major attraction of the patch test is in its simplicity both in concept and in implementation. It offers a simple way to test the convergence of an element without extensive numerical experimentation. Despite doubts about its universal validity (Stummel 1980, Verma and Melosh 1987), examples abound in its successful applications (Razzaque 1986, Taylor *et al.* 1986). A weak patch test was also proposed (Taylor *et al.* 1986, Belytshko and Lasly 1988). This test requires only that the errors be diminished as mesh is refined. A recent study on Mindlin plate elements confirms the usefulness of this test in proving convergence (Park and Choi 1997). Thus, the patch test or its variation remains a useful tool in finite element development. While almost all of the patch test's applications have been on the after-fact assessment of element convergence, there was at least one prominent example of using it in guiding the development of a new element (Taylor *et al.* 1976) twenty years ago. In that study, the integrand in a stiffness formula was altered to meet the requirement of the patch test.

† Professor, Dean; formerly Professor of Civil Engineering, University of Houston, Houston, TX 77204-4791, U.S.A.

At about the same time, a more direct use of patch test in element development was advocated (Bergan and Hanssen 1976). The concept of a single element, instead of a patch, test was advanced. It eventually lead to the use of orthogonal displacement functions for element formulation (Bergan 1980, 1981). In the meanwhile, a separate development based on the single element test concept lead to a vector combination procedure in element formulation (Mau 1982, Mau and Dan 1986). In both the orthogonal function approach and the vector combination approach, it was clearly indicated that passing the higher order test could lead to asymmetric element stiffness matrices. The method proposed to restore symmetry (Mau 1982), however, yielded one type of element which was identical to a restricted form of hybrid stress element and another type which was found to be inferior to the hybrid stress element in numerical experimentation (Mau and Dan 1986). Thus, it appears that such methods are only of theoretical interest.

In this paper, the same concept used by the author in the two previous publications is redeveloped and the procedure used in restoring symmetry of the element stiffness matrix is reexamined. As the formulation unfolds, a natural way of restoring symmetry presents itself. A new type of element results. Preliminary numerical experimentation indicates that a 4-node quadrilateral plane stress element developed with this method out-performs the hybrid stress counterpart. It also does not have the limitations of the nonconforming displacement counterpart. Its implementation is simple and direct, without having to resort to orthogonal functions or vector orthonormalization as proposed before.

2. Basic formulas

It is proposed to design an element which is able to reproduce correctly the desired stress-strain solutions when its nodal displacements are given with the value corresponding to such solutions. In linear elasticity, polynomial general solutions are available if boundary conditions are ignored. Thus, we may use rigid-body, constant strain, linear strain, $\cdots$, modes of these solutions progressively in designing an element. For an N-degree-of-freedom element, we may introduce N modes, including the rigid-body modes. Each of these modes contains a consistent set of displacement-strain-stress functions, $\boldsymbol{u}$-$\boldsymbol{\varepsilon}$-$\boldsymbol{\sigma}$, that satisfy the equilibrium equations. The linear combination of these modes forms the set that contains all representable element responses. The combination coefficients of the N modes are the generalized degrees-of-freedom of the element. Let us denote the vector containing these generalized degrees-of-freedom by $\boldsymbol{D}$, the length of which is N. Corresponding to each component in $\boldsymbol{D}$, there is a set of nodal displacements obtainable from $\boldsymbol{u}$ by specifying the nodal coordinate values in $\boldsymbol{u}$. The collection of the N sets of nodal displacement vectors is denoted by $\boldsymbol{U}$, which contains the rigid-body nodal vectors, $\boldsymbol{U}_o$, the constant strain nodal vectors, $\boldsymbol{U}_c$, and the higher order nodal vectors, $\boldsymbol{U}_h$.

$$\boldsymbol{U} = [\boldsymbol{U}_o \, \boldsymbol{U}_c \, \boldsymbol{U}_h] \tag{1}$$

From the definition of $\boldsymbol{U}$ and $\boldsymbol{D}$, it follows that any nodal displacement vector, Δ, is represented by a linear combination of the vectors in $\boldsymbol{U}$.

$$\Delta_{N\times 1} = \boldsymbol{U}_{N\times N} \, \boldsymbol{D}_{N\times 1} \tag{2}$$

Thus, the matrix $\boldsymbol{U}$ may be called the nodal displacement matrix.

In choosing the modes, care must be taken to ensure that $\boldsymbol{U}$ is not singular. Thus, for any given

nodal displacement vector Δ, the modal coefficients $\boldsymbol{D}$ can be obtained via the inverse of $\boldsymbol{U}$.

$$\boldsymbol{D} = \boldsymbol{U}^{-1}\Delta \tag{3}$$

The matrix $\boldsymbol{U}^{-1}$, a transformation matrix linking Δ to $\boldsymbol{D}$, will be used later in formulating the element stiffness matrix.

From the N sets of displacement-strain-stress solutions, we may express the strain vector in terms of the generalized degrees-of-freedom.

$$\varepsilon = \boldsymbol{BD} \tag{4}$$

where $\boldsymbol{B}$ contains the spatial functions in polynomial forms. The stress vector is then obtained from

$$\sigma = \boldsymbol{E}\,\varepsilon = \boldsymbol{EBD} \tag{5}$$

where $\boldsymbol{E}$ is a symmetric matrix containing the material constants. An intrinsic element stiffness matrix, $\boldsymbol{k}$, can then be defined from the energy expression of the whole element

$$\int \sigma^T \varepsilon\, dV = \boldsymbol{D}^T \int \boldsymbol{B}^T \boldsymbol{EB}\, dV \boldsymbol{D} = \boldsymbol{D}^T \boldsymbol{kD} \tag{6}$$

where

$$\boldsymbol{k} = \int \boldsymbol{B}^T \boldsymbol{EB}\, dV \tag{7a}$$

At this point, it is interesting to point out that using the transformation matrix $\boldsymbol{U}^{-1}$ to relate the generalized degrees-of-freedom, $\boldsymbol{D}$, to the nodal displacements, Δ, would lead to an element stiffness matrix in the form of $(\boldsymbol{U}^T)^{-1}\boldsymbol{kU}$, which is exactly the form of the conventional stiffness matrix. Such an approach would generally lead to nonconverging elements, however, because the solution functions chosen are not necessarily representing conforming displacement fields. Another important point is that each component of $\boldsymbol{k}$ represents the cross-energy of two modes:

$$k_{ij} = \int \sigma_i \varepsilon_j\, dV = \int \sigma_j \varepsilon_i\, dV = k_{ji} \tag{7b}$$

Thus, by virtue of reciprocal theorem, this matrix is inherently symmetric. A third point is that Bergan sought to make this matrix diagonal by selecting fields that were orthogonal to each other (Bergan 1980). It is of course not always easy or even possible to find orthogonal functions to represent useful modes for general element shapes.

The next step is to generate element nodal force vectors from the selected stress solutions. This is done in the same way as that of the hybrid stress method (Pian 1964, Pian and Mau 1972). We interpolate a displacement function along an element boundary using the nodal displacements that uniquely defines the displacement function. The work done by the boundary traction upon the boundary displacement is then equated to the sum of the product of nodal forces and nodal displacements pertaining to that boundary. The result can be expressed in the following form.

$$\boldsymbol{P}_{N\times 1} = \boldsymbol{F}_{N\times N}\boldsymbol{D}_{N\times 1} \tag{8}$$

where $\boldsymbol{P}$ is the element nodal force vecor and the transformation matrix $\boldsymbol{F}$ relates the generalized degrees-of-freedom to the nodal force vector. By generating nodal forces this way, the two sides of a common boundary in an element mesh will generate equal and opposite nodal forces if the stress field is continuous across element boundaries. Thus, under a patch test the nodal forces will cancel each other and the resulting finite element solution will be correct (Bergan 1980, Mau

1982).

We note that each column in $\boldsymbol{F}$ represents the nodal force vector corresponding to a column of nodal displacements in $\boldsymbol{U}$. As such, the matrix $\boldsymbol{F}$ can also be partitioned according to the solution modes.

$$\boldsymbol{F} = [\boldsymbol{F}_o \boldsymbol{F}_c \boldsymbol{F}_h] \tag{9}$$

Obviously $\boldsymbol{F}_o$ are null vectors since they correspond to rigid-body modes. The matrix $\boldsymbol{F}$ will be called nodal force matrix. Now we have all the means to generate the stiffness matrices of three type of converging elements.

3. Type A element

The most desirable element stiffness matrix in terms of accuracy in representing the selected solution modes would be one that satisfies the following equation.

$$\boldsymbol{KU} = \boldsymbol{F} \tag{10}$$

where $\boldsymbol{K}$ is the element stiffness matrix. Such an element will not only pass the patch test for constant strain modes but also will represent the higher order modes correctly. From Eq. (11), the stiffness matrix can be obtained as

$$\boldsymbol{K} = \boldsymbol{FU}^{-1} \tag{11}$$

In actual implementation, we may orthonormalize $\boldsymbol{U}$ by a successive linear combination procedure (Mau 1982) to ensure $\boldsymbol{U}^{-1}=\boldsymbol{U}^T$. Then $\boldsymbol{K}=\boldsymbol{FU}^T$.

We may investigate whether $\boldsymbol{K}$ is symmetric by inserting an identity matrix $\boldsymbol{I}=(\boldsymbol{U}^T)^{-1}\boldsymbol{U}^T$ into the right-hand-side of Eq. (11), regardless whether $\boldsymbol{U}$ is orthonormal or not.

$$\boldsymbol{K} = (\boldsymbol{U}^T)^{-1}\boldsymbol{U}^T\boldsymbol{FU}^{-1} = (\boldsymbol{U}^{-1})^T(\boldsymbol{U}^T\boldsymbol{F})(\boldsymbol{U}^{-1}) \tag{12}$$

Now we see that $\boldsymbol{K}$ will be symmetric if and only if $\boldsymbol{U}^T\boldsymbol{F}$ is symmetric. The matrix $\boldsymbol{U}^T\boldsymbol{F}$, however, represent the cross-energy matrix of the selected solution modes. Thus, it should be identical to the matrix $\boldsymbol{k}$. Referring to Eqs. (6) and (7), it is clear that the matrix $\boldsymbol{k}$ is the result of integration of the energy terms over the element domain. Equivalently, the same can be obtained through an integration over the element boundary, from which the matrix $\boldsymbol{U}^T\boldsymbol{F}$ should result. But $\boldsymbol{F}$ is defined not by integration along the element boundary of the traction upon the "correct" boundary displacements obtained from the selected modes but upon the interpolated displacements uniquely defined by the nodal displacements. This was necessary to ensure the passage of the patch test but in the meantime may have distorted the k_{ij} into $(\boldsymbol{U}^T\boldsymbol{F})_{ij}$. This becomes obvious, if we study the composition of $\boldsymbol{U}^T\boldsymbol{F}$ carefully. We shall denote the matrix $\boldsymbol{U}^T\boldsymbol{F}$ by the Greek letter κ to signify its relation with the matrix $\boldsymbol{k}$. Using Eqs. (1) and (9), we obtain

$$\kappa = \boldsymbol{U}^T\boldsymbol{F} = \begin{bmatrix} \boldsymbol{U}_o^T\boldsymbol{F}_o & \boldsymbol{U}_o^T\boldsymbol{F}_c & \boldsymbol{U}_o^T\boldsymbol{F}_h \\ \boldsymbol{U}_c^T\boldsymbol{F}_o & \boldsymbol{U}_c^T\boldsymbol{F}_c & \boldsymbol{U}_c^T\boldsymbol{F}_h \\ \boldsymbol{U}_h^T\boldsymbol{F}_o & \boldsymbol{U}_h^T\boldsymbol{F}_c & \boldsymbol{U}_h^T\boldsymbol{F}_h \end{bmatrix} \tag{13}$$

From the way $\boldsymbol{F}$ is generated, it is clear that if the displacement of the solution mode along element boundary is of an order equal to or lower than that of the interpolated displacement

function used in generating the nodal forces, then the submatrix in Eq. (13) would be the correct representation of the corresponding term in $\boldsymbol{k}$. Thus, $\boldsymbol{U}_c^T\boldsymbol{F}_h$ would be correct but $\boldsymbol{U}_h^T\boldsymbol{F}_c$ would not because the higher order displacement represented by $\boldsymbol{U}_h$ has been replaced by a lower order interpolated boundary displacement. For example, if along an element boundary there are only two end-nodes and the nodal degrees-of-freedom contain only displacements, then only a linear displacement can be uniquely defined. Any quadratic displacement along the same boundary resulting from a selected mode would lead to a term of $\boldsymbol{U}_h^T\boldsymbol{F}_c$ that is not equal to the corresponding term k_{ij}. Thus, the symmetry of $\boldsymbol{k}$ is destroyed in κ. The asymmetry of the matrix κ is illustrated in Fig. 1a. Here we assume there are three rigid-body modes, three constant strain modes, and two linear strain modes. The first three rows and columns of κ are zeros because (1) the three vectors in $\boldsymbol{F}_o$ are null vectors and (2) the vectors in $\boldsymbol{F}_c$ and $\boldsymbol{F}_h$ are self-equilibrating vectors that produce zero energy when multiplied by the rigid-body nodal displacement vectors, $\boldsymbol{U}_o$. The central part of the matrix, from the fourth to the sixth row and column, representing $\boldsymbol{U}_c^T\boldsymbol{F}_c$, are symmetric, because the constant-strain displacement is of the same order as that of the interpolated boundary displacement. That part of the matrix in columns and rows seven and eight, representing $\boldsymbol{U}_c^T\boldsymbol{F}_h$, $\boldsymbol{U}_h^T\boldsymbol{F}_c$ and $\boldsymbol{U}_h^T\boldsymbol{F}_h$ are generally asymmetric. Thus, this type of element will have asymmetric stiffness matrix in general but it will pass the constant strain patch test and will represent higher order solution modes correctly. This element is called Type A element.

4. Type S element

It is desirable to have symmetric stiffness matrices for computational reasons. From the above investigation of the symmetry of κ, it may be concluded that the last column and the last row of submatrices in the expression of Eq. (13) are generally the source of asymmetry. We may change either the columns in $\boldsymbol{F}$ or the columns in $\boldsymbol{U}$ corresponding to the higher order modes such that the resulting κ is symmetric. In either way, the changed $\boldsymbol{F}$ or $\boldsymbol{U}$ no longer represent the originally selected high order modes correctly and the resulting stiffness matrix will not pass the higher order patch test. Since the constant strain modes are not affected, however, the basic patch test will still be passed.

Let us use Fig. 1 to explain the process of restoring symmetry in the matrix κ. We consider the case of changing the linear-strain-mode nodal displacements $\boldsymbol{U}_h$, represented by $\boldsymbol{U}_7$ and $\boldsymbol{U}_8$. The effect of any changes in these two nodal displacement vectors is to change the seventh and the eighth rows in κ. Mathematically there are infinite possibilities to change these two vectors such that the resulting seventh and eighth rows of κ would make a symmetric κ. We propose to use only linear combination of the nodal displacement vectors of the constant strain modes to effect the change of the linear-strain-mode displacement vectors and we change them one vector at a time. Thus,

$$\boldsymbol{U}_7' = \boldsymbol{U}_7 + a\boldsymbol{U}_4 + b\boldsymbol{U}_5 + c\boldsymbol{U}_6 \tag{14}$$

where $\boldsymbol{U}_7'$ is the new nodal displacement vector, and the combination coefficients, a, b, and c are to be solved from the following equation,

	F1	F2	F3	F4	F5	F6	F7	F8
U1	0	0	0	0	0	0	0	0
U2	0	0	0	0	0	0	0	0
U3	0	0	0	0	0	0	0	0
U4	0	0	0	κ_{44}	κ_{45}	κ_{46}	κ_{47}	κ_{48}
U5	0	0	0	κ_{45}	κ_{55}	κ_{56}	κ_{57}	κ_{58}
U6	0	0	0	κ_{46}	κ_{56}	κ_{66}	κ_{67}	κ_{68}
U7	0	0	0	κ_{74}	κ_{75}	κ_{76}	κ_{77}	κ_{78}
U8	0	0	0	κ_{84}	κ_{85}	κ_{86}	κ_{87}	κ_{88}

(a)

$\rightarrow$

	F1	F2	F3	F4	F5	F6	F7	F8
U1	0	0	0	0	0	0	0	0
U2	0	0	0	0	0	0	0	0
U3	0	0	0	0	0	0	0	0
U4	0	0	0	κ_{44}	κ_{45}	κ_{46}	κ_{47}	κ_{48}
U5	0	0	0	κ_{45}	κ_{55}	κ_{56}	κ_{57}	κ_{58}
U6	0	0	0	κ_{46}	κ_{56}	κ_{66}	κ_{67}	κ_{68}
U7	0	0	0	κ_{47}	κ_{57}	κ_{67}	κ_{77}'	κ_{78}'
U8	0	0	0	κ_{84}	κ_{85}	κ_{86}	κ_{87}	κ_{88}

(b)

$\rightarrow$

	F1	F2	F3	F4	F5	F6	F7	F8
U1	0	0	0	0	0	0	0	0
U2	0	0	0	0	0	0	0	0
U3	0	0	0	0	0	0	0	0
U4	0	0	0	κ_{44}	κ_{45}	κ_{46}	κ_{47}	κ_{48}
U5	0	0	0	κ_{45}	κ_{55}	κ_{56}	κ_{57}	κ_{58}
U6	0	0	0	κ_{46}	κ_{56}	κ_{66}	κ_{67}	κ_{68}
U7	0	0	0	κ_{47}	κ_{57}	κ_{67}	κ_{77}'	κ_{78}'
U8	0	0	0	κ_{48}	κ_{58}	κ_{68}	κ_{78}'	κ_{88}'

(c)

Fig. 1 (a) The asymmetric matrix created from the matrices U and F; (b) after correction by changing U_7; (c) after correction by changing U_8; bold-face part is symmetric

$$\begin{bmatrix} \kappa_{44} & \kappa_{45} & \kappa_{46} \\ \kappa_{45} & \kappa_{55} & \kappa_{56} \\ \kappa_{46} & \kappa_{56} & \kappa_{66} \end{bmatrix} \begin{Bmatrix} a \\ b \\ c \end{Bmatrix} = \begin{Bmatrix} \kappa_{47}-\kappa_{74} \\ \kappa_{57}-\kappa_{75} \\ \kappa_{67}-\kappa_{76} \end{Bmatrix} \tag{15}$$

so that when U_7' replaces U_7, the corrsponding change (addition) in κ would be such that the fourth, fifth, and sixth components in row seven of κ become κ_{47}, κ_{57} and κ_{67}, respectively, Fig. 1b. The remaining components in row 7, κ_{77} and κ_{78} are changed accordingly.

$$\kappa_{77}' = \kappa_{77} + a\,\kappa_{47} + b\,\kappa_{57} + c\,\kappa_{67} \tag{16a}$$

$$\kappa_{78}' = \kappa_{78} + a\,\kappa_{48} + b\,\kappa_{58} + c\,\kappa_{68} \tag{16b}$$

The same procedure is now repeated for U_8 but with four vectors involved.

$$U_8' = U_8 + dU_4 + eU_5 + fU_6 + gU_7' \tag{17}$$

$$\begin{bmatrix} \kappa_{44} & \kappa_{45} & \kappa_{46} & \kappa_{47} \\ \kappa_{45} & \kappa_{55} & \kappa_{56} & \kappa_{57} \\ \kappa_{46} & \kappa_{56} & \kappa_{66} & \kappa_{67} \\ \kappa_{47} & \kappa_{57} & \kappa_{67} & \kappa_{77}' \end{bmatrix} \begin{Bmatrix} d \\ e \\ f \\ g \end{Bmatrix} = \begin{Bmatrix} \kappa_{48}-\kappa_{84} \\ \kappa_{58}-\kappa_{85} \\ \kappa_{68}-\kappa_{86} \\ \kappa_{78}'-\kappa_{87} \end{Bmatrix} \tag{18}$$

$$\kappa_{88}' = \kappa_{88} + d\,\kappa_{48} + e\,\kappa_{58} + f\,\kappa_{68} + g\,\kappa_{78}' \tag{19}$$

As a minor point, it is noted that in the above computation for the combination coefficients, only symmetric matrices are involved in the solution, making the implementation easy. With the change implemented, the resulting new matrix κ' is now symmetric. It is observed, however, that this new matrix κ' is not identical to $\boldsymbol{k}$. Aside from the $U_h^T F_h$ terms, however, the rest of κ are identical to $\boldsymbol{k}$.

The above procedure departs from that previously proposed by Mau (1982) in a critical point. In that previous work, it was proposed to use the combination of constant-strain and linear-strain displacement vectors, U_c and U_h, for the new U_h, such that the resulting matrix κ is identical to $\boldsymbol{k}$.

As we shall see in the next section, this invariably leads to a hybrid stress element. The current procedure does create a new type of element which is potentially more robust than the hybrid stress element as shall be shown by an numerical example later.

Having obtained the new matrix U', the element stiffness matrix is calculated by

$$K = F(U')^{-1} \tag{20}$$

An alternative procedure to restore the symmetry of κ is by changing F_h. Since F_h affects the last columns, columns 7 and 8, of κ, we must then use the corresponding values in the rows as the target value in seeking the coefficients of combination so that the changed values in the columns would match those from the rows. The procedure proposed herein is parallel to that for the U_h and can be summarized for F_7' in the following three equations.

$$F_7' = F_7 + a'F_4 + b'F_5 + c'F_6 \tag{21}$$

$$\begin{bmatrix} \kappa_{44} & \kappa_{45} & \kappa_{46} \\ \kappa_{45} & \kappa_{55} & \kappa_{56} \\ \kappa_{46} & \kappa_{56} & \kappa_{66} \end{bmatrix} \begin{Bmatrix} a' \\ b' \\ c' \end{Bmatrix} = - \begin{Bmatrix} \kappa_{47} - \kappa_{74} \\ \kappa_{57} - \kappa_{75} \\ \kappa_{67} - \kappa_{76} \end{Bmatrix} \tag{22}$$

$$\kappa_{77}' = \kappa_{77} + a'\kappa_{74} + b'\kappa_{75} + c'\kappa_{76} \tag{23}$$

The formula for F_8 would be parallel to Eqs. (17)-(19) and need not be shown here. With the new F' obtained, the element stiffness matrix is calculated by

$$K = F'U^{-1} \tag{24}$$

Again, this procedure departs from a previous one proposed by Mau (1982) in the same way described for the case of changing U. The previous procedure was shown to lead to an element that was inferior to the hybrid stress element in numerical experimentation (Mau and Dan 1986).

The resulting new κ' according to the current procedure is in general different from both k and the κ' associated with a changed U. Intuitively, it seems to suggest that the element stiffness matrices calculated from Eqs. (20) and (24) are quite different. Thus, it is surprising, when numerical experimentation is carried out, to find that the two element stiffness matrices are actually identical. Upon further investigation, however, it becomes clear that they should indeed be identical to each other. We first note that, by comparing Eq. (15) with Eq. (22), the combination coefficents for the Us in Eq. (14) differ from those for the Fs in Eq. (21) by only a negative sign. Thus, Eq. (21) can be rewritten as

$$F_7' = F_7 - aF_4 - bF_5 - cF_6 \tag{21a}$$

with a similar formula for F_8'. Let us concentrate only on F_7'. The pair of vectors F_7' and U_7, which are used in Eq. (24) to calculate the element stiffness matrix K, can be modified by the following formula without having any effect in the resulting K.

$$F_7'' = F_7' + aF_4 + bF_5 + cF_6 \tag{25a}$$

$$U_7'' = U_7 + aU_4 + bU_5 + cU_6 \tag{25b}$$

This is because adding corresponding pairs of F_4-U_4, F_5-U_5, and F_6-U_6, to the pair F_7'-U_7, does not change the conditions on K as represented in Eq. (10). Thus, the two pairs, F_7'-U_7 and F_7''-U_7'' would yield the same K, other conditions being equal. But the pair F_7''-U_7'' is nothing but the

same pair F_7-U_7', according to Eqs. (14), (21a), and (25). A similar argument can be made for the pair of F_8'-U_8 and F_8''-U_8''. Thus, Eq. (24) would yield the same symmetrical K as Eq. (20). Henceforth, this element is called Type S element.

As a final note on the subject of identical stiffness matrices, we would arrive at yet another identical stiffness matrix if we choose to change both U_h and F_h, such that the resulting new κ has components in the last columns and rows made to equal the average of the original values. The proof is similar to the one just presented.

5. Type H element

In all the currently suggested procedures that lead to identical symmetric element stiffness matrices, the resulting energy matrices, κ, are all different from the original k, obtained from integration over the element domain, Eq. (7). Wouldn't it be nice if we can change U_h or F_h, such that resulting κ is identical to k? This of course was the original intent in the work published before (Mau 1982, Mau and Dan 1986). The answer is already outlined in Section 4. That is, by changing just U_h and leave F intact, it is possible to make κ identical to k. The procedure was given by Mau (1982) and need not be repeated herein. Let us denote the changed U by $\overline{U}$. Then,

$$K = F\overline{U}^{-1} \tag{26}$$

where the new displacement vectors $\overline{U}$ satisfy the following condition

$$\overline{U}^T F = F^T \overline{U} = k \tag{27}$$

We shall now prove that this element stiffness matrix is identical to the hybrid stress element stiffness matrix obtained from the same assumed stress modes. We shall prove this statement in two steps. First, we shall put the hybrid stress element stiffness matrix into the present context. The hybrid stress formulation contains two key matrices, H, and G (Pian 1964) and the element stiffness matrix K_H is calculated by

$$K_H = GH^{-1}G^T \tag{28}$$

The H matrix is identifiable from the energy expression obtained by integration over the element domain in the current formulation.

$$\int \sigma^T \varepsilon dV = \int \sigma^T E^{-1} \sigma dV = D^T \int B^T E E^{-1} E B dV\, D = D^T k D \tag{29}$$

Thus, H is contained in k. Since k includes the zero-energy contributions from the rigid-body modes, we can identify H as the nonzero part of the matrix k.

$$k = \begin{bmatrix} 0 & 0 \\ 0 & H \end{bmatrix} \tag{30}$$

The G matrix relates the stress parameters to the nodal forces. Since in the current formulation the stress parameters are represented also by D as shown in Eq. (5) ($\sigma = E\varepsilon = EBD$), the G matrix is identical to the nonzero part of matrix F in the current formulation, according to Eq. (9).

$$F = [0 \;\; G] \tag{31}$$

where, $G=[F_c \;\; F_h]$. Let us define

$$\bar{k} = \begin{bmatrix} 0 & 0 \\ 0 & H^{-1} \end{bmatrix} \tag{32}$$

Then,

$$F\bar{k}F^T = [0 \;\; G] \begin{bmatrix} 0 & 0 \\ 0 & H^{-1} \end{bmatrix} \begin{bmatrix} 0 \\ G^T \end{bmatrix} = GH^{-1}G^T$$

Thus, the stiffness matrix of an assumed stress hybrid element can be expressed as

$$K_H = F\bar{k}F^T \tag{33}$$

This completes the first step.

We now proceed to show that

$$K_H \bar{U} = F \tag{34}$$

This is achieved by successive substitution using Eqs. (33), (32), (27), and (30).

$$K_H \bar{U} = F\bar{k}F^T\bar{U} = F \begin{bmatrix} 0 & 0 \\ 0 & H^{-1} \end{bmatrix} F^T\bar{U} = F \begin{bmatrix} 0 & 0 \\ 0 & H^{-1} \end{bmatrix} \begin{bmatrix} 0 & 0 \\ 0 & H \end{bmatrix}$$

$$= F \begin{bmatrix} 0 & 0 \\ 0 & I \end{bmatrix} = [0 \;\; G] \begin{bmatrix} 0 & 0 \\ 0 & I \end{bmatrix} = [0 \;\; G] = F \tag{35}$$

Thus, the K_H is identical to the K in Eq. (26). This completes the proof. This element is called Type H element.

6. Implementation summary

To generate the three types of element stiffness matrices numerically, the first step is to select a set of polynomial general solutions, whose number matches that of the element degrees-of-freedom, N. From these solutions, the nodal force and nodal displacement matrices F and U containing the N pairs of nodal displacements and nodal forces are generated. Eq. (11) can then be used to generate K of the Type A element. The inversion of U can be avoided if U is orthonormalized (and the F adjusted accordingly).

For Type S elements, we first generate the matrix $\kappa = U^T F$. This matrix is made to be symmetric by finding the new U' by Eqs. (14) through (19). Then K is calculated by Eq. (20). Again orthonomalization can be used to simplify the computation.

For Type H elements, i.e., the hybrid stress elements with assumed stress field also satisfying compatibility, there is no need to find U. Rather the matrix k (actually only the nonzero part, H) is calculated through integration over the element domain. K is then calculated via Eq. (33).

The computational procedure for all three types of elements is unified if we use the same stiffness matrix expression for all three elements.

$$K = GH^{-1}G^T \tag{36}$$

where G and H are defined by

$$F = [0 \;\; G], \qquad U^T F = \begin{bmatrix} 0 & 0 \\ 0 & H \end{bmatrix} \quad \text{for Type A element} \tag{37a}$$

$$F = [0 \;\; G], \qquad (U')^T F = \begin{bmatrix} 0 & 0 \\ 0 & H \end{bmatrix} \quad \text{for Type S element} \tag{37b}$$

$$F = [0 \;\; G], \qquad k = \begin{bmatrix} 0 & 0 \\ 0 & H \end{bmatrix} \quad \text{for Type H element} \tag{37c}$$

7. Numerical examples

We will use three examples to investigate the robustness of the three types of elements in the case of a 4-node plane stress quadrilateral.

First, the basic formulas are described. The chosen solution functions for displacements, strains and stresses, in a Cartesian coordinate system x-y, are

$$\begin{Bmatrix} u \\ v \end{Bmatrix} = \begin{bmatrix} 1 & 0 & -y & x & -\mu x & \frac{y}{2} & xy & -\frac{\mu x^2 + y^2}{2} \\ 0 & 1 & x & -\mu y & y & \frac{x}{2} & -\frac{x^2 + \mu y^2}{2} & xy \end{bmatrix} D \tag{38}$$

$$\begin{Bmatrix} \varepsilon_{xx} \\ \varepsilon_{yy} \\ \varepsilon_{xy} \end{Bmatrix} = \begin{bmatrix} 0 & 0 & 0 & 1 & -\mu & 0 & y & -\mu x \\ 0 & 0 & 0 & -\mu & 1 & 0 & -\mu y & x \\ 0 & 0 & 0 & 0 & 0 & 1 & 0 & 0 \end{bmatrix} D \tag{39}$$

and

$$\begin{Bmatrix} \sigma_{xx} \\ \sigma_{yy} \\ \sigma_{xy} \end{Bmatrix} = \begin{bmatrix} 0 & 0 & 0 & E & 0 & 0 & Ey & 0 \\ 0 & 0 & 0 & 0 & E & 0 & 0 & Ex \\ 0 & 0 & 0 & 0 & 0 & G & 0 & 0 \end{bmatrix} D \tag{40}$$

From Eq. (38), we obtain

$$\Delta = UD$$

where

$$\Delta = [u_1 \; v_1 \; u_2 \; v_2 \; u_3 \; v_3 \; u_4 \; u_4]$$
$$D = [D_1 \; D_2 \; D_3 \; D_4 \; D_5 \; D_6 \; D_7 \; D_8]$$

and the 8x8 matrix U is defined by the following equation, which shows only the contribution

from the ith node with x_i and y_i representing the nodal coordinates.

$$\begin{Bmatrix} u_i \\ v_i \end{Bmatrix} = \begin{bmatrix} 1 & 0 & -y_i & x_i & -\mu x_i & \dfrac{y_i}{2} & x_i y_i & -\dfrac{\mu x_i^2 + y_i^2}{2} \\ 0 & 1 & x_i & -\mu y_i & y_i & \dfrac{x_i}{2} & -\dfrac{x_i^2 + \mu y_i^2}{2} & x_i y_i \end{bmatrix} \boldsymbol{D} \tag{41}$$

The matrix $\boldsymbol{F}$ is obtained by integration over each side of the element using the traction calculated from Eq. (40) and a linear displacement defined by the two end-nodes of that side. The results from all four sides constitute the equation $\boldsymbol{P}=\boldsymbol{FD}$.

In the following equation, the contribution from a typical side i-j is show.

$$\begin{Bmatrix} \boldsymbol{P}_{2i-1} \\ \boldsymbol{P}_{2i} \\ \boldsymbol{P}_{2j-1} \\ \boldsymbol{P}_{2j} \end{Bmatrix} = \begin{bmatrix} 0 & 0 & 0 & \dfrac{y_{ji}E}{2} & 0 & \dfrac{-x_{ji}G}{2} & \dfrac{y_{ji}(y_j+2y_i)E}{6} & 0 \\ 0 & 0 & 0 & 0 & \dfrac{-x_{ji}E}{2} & \dfrac{y_{ji}G}{2} & 0 & \dfrac{-x_{ji}(x_j+2x_i)E}{6} \\ 0 & 0 & 0 & \dfrac{y_{ji}E}{2} & 0 & \dfrac{-x_{ji}G}{2} & \dfrac{y_{ji}(y_j+2y_i)E}{6} & 0 \\ 0 & 0 & 0 & 0 & \dfrac{-x_{ji}E}{2} & \dfrac{y_{ji}G}{2} & 0 & \dfrac{-x_{ji}(x_i+x_j)E}{6} \end{bmatrix} \boldsymbol{D} \tag{47}$$

where $x_{ji}=x_j-x_i$, $y_{ji}=y_j-y_i$, and $j=i+1$, with $i=1$, 2, 3, 4 and j runs between 1 and 4 cyclically. From here on the three types of element stiffness matrices can be programmed easily.

The first numerical example is a set of test problems containing two basic patch tests and a higher order patch test shown in Fig. 2. For the basic tension and shear tests, all three elements, Type A, Type S, and Type H, produce the exact answers. The bending test, however, is a higher order test. Only the Type A asymmetric element produces the exact answer as expected. The Type S element gives 76.7% of the correct transverse displacement at the right edge and 88.6% of the correct tensile stress at the right upper corner while the corresponding numbers for the Type H element are 85.0% and 141.0% respectively. The Type H element is identical to the 5-parameter assumed stress hybrid element (Pian 1964).

The second numerical example is for the bending of a cantilever beam. The meshes used and

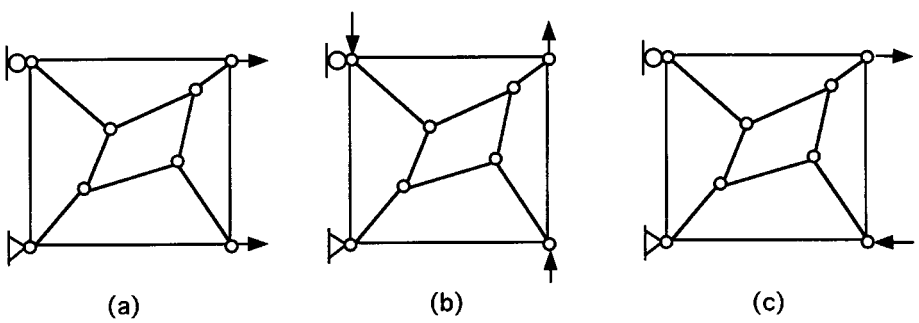

Fig. 2 Basic patch test for (a) tension and (b) shear, and (c) higher order patch test for bending; all loads are of equal magnitude

Table 1 Accuracy of the Type S and the Type H elements

Finite element mesh	Quantity	Type S	Type H
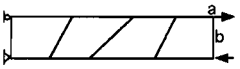	Deflection at b	94.5%	88.3%
	Tension at a	107.2%	105.2%
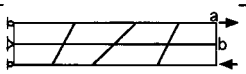	Deflection at b	97.6%	72.8%
	Tension at a	96.5%	86.8%
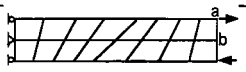	Deflection at b	99.3%	96.3%
	Tension at a	102.5%	102.6%

the results are given in Table 1. Not shown are the results of the Type A element because they are all 100% of the exact value as expected. As far as this kind of problems are concerned, the Type S element seems to be more accurate than the Type H element.

It is interesting to point out that the mesh is chosen so that a comparison with the result obtained from the nonconforming 4-node quadrilateral element (Taylor, Beresford and Wilson 1976) can be made. In a separate publication (Taylor *et al.* 1986) the result of the nonconforming element for the 8-element mesh in Table 1 is given. Using a reduced 2×2 numerical integration, the nonconforming element produced 97.5% of the correct deflection at point *b*. Thus, the Type S element is similar in accuracy to the nonconforming element. However, if a 3×3 integration were used, the result would be only 91.6%. In addition, both integration schemes produced elements that were sensitive to the Poisson's ratio approaching 0.5 (Taylor *et al.* 1986). The current Type S element does not depend on reduced integration schemes and also displays no such sensitivity.

The third example is the plane stress problem shown in Table 2, with a unit load distributed uniformly at the right end. This was the problem used to test the accuracy of several new elements (Cook 1974) and the nonconforming element commonly named as QM6 (Taylor, Beresford and Wilson 1976) in the early years of finite element development. The problem was popularized by a well known textbook on finite element methods (Cook, Malkus and Plesha 1989). It is a difficult problem because obviously both bending and shear actions are important. Since the elements studied in this paper are designed for bending representation, it is useful to see how well they fare with this particular problem. In this application, the displacement-stress-strain fields are referred to a local coordinate system using one side of an element as one of the coordinate axes. This is similar to but simpler than the local coordinate system adopted by Cook (1974). The results for the three types of elements, Types A, S, and H, as well as the result of QM6 element

Table 2 Accuracy of the Type A, Type S and Type H elements

Finite element mesh	Quantity	Type A	Type S	Type H	QM6*
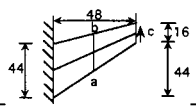	Deflection at c	88.0%	90.4%	68.3%	88.4%
	Min. stress at b	66.4%	74.9%	51.4%	78.8%
	Max. stress at a	74.0%	88.7%	69.2%	84.0%
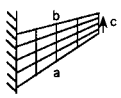	Deflection at c	96.1%	96.6%	89.1%	96.7%
	Min. stress at b	90.9%	94.5%	80.9%	92.6%
	Max. stress at a	93.2%	97.3%	90.3%	97.8%

*Taylor, Beresford and Wilson (1976)

reported by Taylor, Beresford, and Wilson (1976) are summarized in Table 2. The Young's modulus and Poisson's ratio are 1 and 1/3, respectively. It is most interesting to see that the Type S element out-performs even the Type A element. This is because the Type A element no longer has the advantage of accurately representing the bending when shear is also important. The Type S element also gives results as good as or slightly better than those from the QM6 element, generally regarded as one of the most robust plane stress elements.

What these limited number of examples have shown is not that the Type S element is the most robust element of all, but rather the possibility of using the proposed method to generate new elements with desirable features. It is quite possible that, instead of starting from the two bending modes as is done herein, one may seek a combination of bending and shear modes for an even more robust element.

8. Discussions

Using the present formulation as basis, the conventional displacement formulation and the hybrid stress formulation can be derived. It is also easy to see why the conventional conforming elements and the hybrid stress elements are convergent elements.

If the displacement field chosen is conforming, its boundary displacement is by definition uniquely determined by its associated nodal displacements. Thus, the energy matrix $\boldsymbol{k}$ is correctly reproduced by the matrix κ. Using the formulation for the Type A element, we will obtain a symmetric element stiffness matrix. It can be shown easily that this element is identical to the conventional displacement element. In this case, we need only a displacement field to form the matrix $\boldsymbol{U}$ and the element stiffness matrix can be obtained from $\boldsymbol{K}=(\boldsymbol{U}^{-1})^T\kappa(\boldsymbol{U}^{-1})$, according to Eqs. (12) and (13). This formula is identical to the conventional displacement element formula. The convergence of this type of elements is based on the fact that as long as the constant strain modes are included on the conforming displacement field, the resulting constant stresses of these modes are always in equilibrium. The corresponding nodal force vectors, $\boldsymbol{F}_c$, will also be in equilibrium and be correctly represented. Thus, the element will always pass the basic patch test. However, because the higher order modes in the chosen displacement field may not correspond to any stress field, since in the conventional approach the only requirement is a continuous displacement field, the nodal force vectors $\boldsymbol{F}_h$ in general will not be meaningful, let alone correct. This may explain why the conforming 4-node quadrilateral element is such a poor element.

Following the Type H element formulation, we can see that it is only necessary to have a stress field that satisfies the equilibrium conditions because we do need to have the resulting $\boldsymbol{F}$ in self-equilibrium. Since Eq. (37c) does not include $\boldsymbol{U}$, we need not have an explicit displacement field over the element domain. This is then the hybrid stress formulation. The constant stress modes in the hybrid stress formulation always correspond to a continuous displacement field. Thus, while the higher order stress modes may not satisfy the compatibility conditions, the constant stress modes always do. As a result, a hybrid stress element containing the constant stress modes will always pass the basic patch test. Again, since the higher order stress modes may not satisfy the compatibility conditions, we cannot in general find a meaningful $\boldsymbol{U}_h$. Intuitively, then, a hybrid stress element with all modes satisfying compatibility may be better. This is called restricted hybrid stress formulation (Mau and Dan 1986). The Type H element belongs to this class of hybrid stress elements.

As a final point of discussion, all three types of elements become one when the element

geometry is such that the asymmetry in κ disappears. This happens for the 4-node quadrilateral when it becomes a rectangular element.

9. Conclusions

A simplified formulation has been developed for the generation of stiffness matrix of convergent elements using element patch test. A new class of elements, Type S, is proposed. Numerical examples have shown that a 4-node plane stress quadrilateral element of this type is robust when compared with a displacement based nonconforming element and a hybrid stress element. The method of formulation can be viewed as a useful alternative to both the displacement formulation and the hybrid stress formulation.

References

Bazeley, G.P., Cheung, Y.K., Irons, B.M., and Zienkiewicz, O.C. (1966), "Triangular elements in plate bending. Conforming and nonconforming solutions", *Proc. 1st Matrix Methods in Struct. Mech.*, AFFDL-TR-CC-80, Wright Patterson, A. F. Base, Ohio, 547-576.

Belytshko, T. and Lasly, S. (1988), "A fractal patch test", *Int. J. Numer. Methods Eng.*, **26**, 2199-2210.

Bergan, P.G. and Hanssen, L. (1976), "A new approach for deriving 'good' element stiffness matrices", *Math. of Finite Elements and Appl.* (Ed. Whiteman, J.R.), Academic Press, London, 483-497.

Bergan, P.G. (1980), "Finite elements based on energy orthogonal functions", *Int. J. Numer. Methods Eng.*, **15**, 1541-1555.

Bergan, P.G. (1981), "Correction and further discussion of 'finite element based on energy orthogonal functions'", *Int. J. Numer. Methods Eng.*, **17**, 154-155.

Cook, R.D. (1974), "Improved two-dimensional finite element", *J. Structural Div., ASCE*, **100**, 1851-1863.

Cook, R.D., Malkus, D.S. and Plesha, M.E. (1989), *Concepts and Applications of Finite Element Analysis*, Third Ed., John Wiley & Sons, New York.

Irons, B.M. and Razzaque, A. (1972), "Experience with the patch test for convergence of finite element methods", *Math. Foundations of the Finite element Method* (Ed. Aziz, A.K.), Academic Press, 557-587.

Mau, S.T. (1982), "A direct vector combination procedure for finite element stiffness matrix formulation", *Int. J. Numer. Methods Eng.*, **18**, 863-878.

Mau, S.T. and Dan H.C. (1986), "A restricted hybrid stress formulation based on a direct finite element method", *Int. J. Numer. Methods Eng.*, **23**, 1495-1507.

Park, Y.M. and Choi, C.K. (1997), "The patch test and convergence for nonconforming Mindlin plate bending elements", *Int. J. Struct. Eng. Mech.*, **5**, 471-490.

Pian, T.H.H. (1964), "Derivation of element stiffness matrices by assumed stress distributions", *AIAA J.*, **2**, 1332-1336.

Pian, T.H.H. and Mau, S.T. (1972), "Some recent studies in assuming stress hybrid models", *Advances in Computational Methods in Structural Mechanics and Design* (Ed. Oden, J.T.), University of Alabama Press, Huntsville, Alabama, 87-106.

Razzaque, A. (1986), "The patch test for elements", *Int. J. Number. Methods Eng.*, **22**, 63-71.

Stummel, F. (1980), "The limitations of the patch test", *Int. J. Numer. Methods Eng.*, **15**, 177-188.

Taylor, R.L., Beresford, P.J. and Wilson, E.L. (1976), "A nonconforming element for stress analysis", *Int. J. Numer. Methods Eng.*, **10**, 1211-1219.

Taylor, R.L., Simo, J.C., Zienkiewicz, O.C. and Chan, A.C.H. (1986), "The patch test-A condition for assessing FEM convergence", *Int. J. Numer. Methods Eng.*, **22**, 39-62.

Verma, A. and Melosh, R.J. (1987), "Numerical test for assessing finite element model convergence", *Int. J. Numer. Methods Eng.*, **24**, 843-857.